JOURNAL OF APPLIED ELECTROCHEMISTRY **28** (1998) 873–880

Selective electrosynthesis of *p*-methoxybenzaldehyde at spinel type $CoMn_2O_4$/titanium-composite anodes*

E. LODOWICKS, F. BECK

University of Duisburg, Fachgebiet Elektrochemie, Lotharstr. 1, D-47057 Duisburg, Germany

Received 21 May 1997; revised 11 September 1997

Activated titanium anodes with a spinel coating of $CoMn_2O_4$ of about 1 μm thickness were developed. A relative stability in acid electrolytes was found. The novel anode was employed for the anodic oxidation of *p*-methoxytoluene (PMT) to *p*-methoxybenzaldehyde (PMB), which is of industrial interest. Batch type electrolyses with 30% theoretical conversion (4 F mol^{-1}) were used for a parametric screening. The solvent/electrolyte-system was 1 M H_2SO_4/5 M H_2O in methanol. Optimum results (60% selectivity, 50–60% current efficiency) were obtained at low concentrations of the educt (0.2 M). A part of the current is consumed for the formation of the benzylmethylether, which can be further oxidized to PMB. It was proved that the novel anode operates according to the mechanism of heterogeneous redox catalysis with ter- and heptavalent manganese as the redox species. A turnover factor of >2000 is unusual for a spinel in acid solution.

Keywords: *organic electrosynthesis*, *p-methoxybenzaldehyde*, *p-methoxytoluene*, *cobalt manganese spinel*, *titanium composite anodes*, *heterogeneous redoxcatalysis*

1. Introduction

Benzaldehyde and its paraderivatives are important organic intermediates. They can be synthesized by direct anodic oxidation of the corresponding toluenes, even at an industrial scale [1–5]. This electrosynthesis is superior to the traditional chemical routes via chlorine chemistry, where benzalchlorides play an important role as intermediates. However, the full potential of this opportunity is not yet realized at classical anode materials like carbon, lead dioxide or platinum due to the formation of acetales as intermediates [1–5] or due to the application of dissolved oxidants like Mn^{3+} or Ce^{4+} in relative dilute electrolytes [2]. The optimum strategy would be the utilization of a selective anode with an appropriate surface fixed oxidic redox system. Beer has demonstrated titanium to be a highly feasible base material for this purpose [6]. Ti/RuO_2-composite anodes with a variety of other oxides like TiO_2, SnO_2, Sb_2O_3 or IrO_2 have been employed for many years as chlorine or oxygen anodes.

These oxides have no advantage for anodic oxidation in organic chemistry due to their low O_2- and Cl_2-overvoltage. But other oxides like Cr_2O_3 [7] do overcome this problem. Previous work on Mn-systems as specific redoxmediators in electroorganic oxidations demonstrated the feasibility of ceramic or electrodeposited MnO_2-layers [8], of electrogenerated MnO_2 slurries [9] and of the redox couple Mn^{2+}/Mn^{3+} [10, 11]. From a historical point of view, it should be mentioned, that Eberson and Nyberg [12, 13] initiated the direct acetoxylation route of toluene (derivatives) at platinum and carbon anodes. Anodic methoxylation at the same anodes in methanolic electrolytes, containing $LiBF_4$ or NaOMe, was described by Ronlán *et al.* [14].

Recently, the relative stability of Ti/$CoMn_2O_4$ anodes of the spinel type was demonstrated for simple electroorganic model reactions such as isopropanol → acetone in acid solutions [15].

$$CH_3{-}CHOH{-}CH_3 \longrightarrow CH_3{-}CO{-}CH_3 + 2H^+ + 2e^- \quad (1)$$

In the present paper the application of these novel anodes for the more interesting oxidation mentioned above is shown [16].

2. Experimental details

Chemicals for electrolyte preparation were analytical grade. H_2SO_4 (95–97%), acetonitrile, methanol and isopropanol were from Riedel de Haën. Organic compounds as the starting material, 4-methylanisol, *p*-methoxytoluene (PMT) (Merck) and standards for GC such as 4-methoxybenzaldehyde (PMB) (Merck), 4-*tert*-butylbenzaldehyde (Lancaster) and others were generally of 98–99% purity.

The preparative anodes were 50 mm × 50 mm × 1 mm sheets of titanium (Thyssen A.G., Krefeld, Contimet 35^{TM}). A current lead of 10 mm × 50 mm was cut at the middle of one side. The quadratic electrode areas were cleaned and degreased and

* Dedicated to Professor Dr. Hans Schäfer on the occasion of his 60th birthday.

0021-891X

etched for 15 min in boiling 5 M HCl. The subsequent activation of both sides was performed through the Mn- and Co-nitrates in methanol (0.05 M/0.025 M, 10 μl cm^2), drying at 100 °C (10 min) and firing in air at 350 °C (10 min). After six thermal cycles, a nominal layer thickness of the $CoMn_2O_4$-spinel of 0.62 μm was attained, assuming a density of 5 g cm^{-3}. Further details of the anode preparation was found in [15, 16].

The divided preparative electrolysis cell was a glass cylinder with a planar ground joint cover. The two counter electrodes were made of stainless steel and were arranged at both sides (d = 3 cm) of the working electrode described above. They were located within two cylindric microporous Al_2O_3-diaphragms 30 mm × 100 mm. In some cases quasi divided cells were employed [5, 7]. The microporous Al_2O_3-diaphragms were omitted, and small area wire counter electrodes (0.5 mm diam.) were arranged at both sides of the anode. The standard conditions for the batch type electrolyses were as follows: j = 2.5 mA cm^{-2}, anolyte composition: 1 M H_2SO_4, 5 M H_2O, 1 M PMT in methanol. Theoretical conversion (4 F mol^{-1}) β_{th} = 30%, initial batch volume = 0.5 dm^3, T = 23 °C, magnetic stirring in the anolyte. The catholyte was 1 M H_2SO_4.

Product analysis was performed through 10 ml samples, which were neutralized with 10–12 ml 2 M NH_3/H_2O to pH 8. The methanol was stripped. The residual was extracted four times with Et_2O (each 10 ml). The unified ether extracts were dried, the inner standard was added (4-*tert*-butyltoluene in the case of anodic oxidation of PMT, benzophenone for the oxidation of 4-*tert*-butyltoluene) and Et_2O was added up to 50 ml. 0.8 μl of this solution were introduced into the gas chromatograph (HP 5880A, 100–250 °C, 25 m glass capillary column, inner diameter 0.31 mm, coating with crosslinked methyl silicone with 5% phenyl groups). Nitrogen was used as a carrier gas with a flow rate of 20 ml min^{-1}. Retention times for known components are shown in Table 2. Reference samples are used for the classification of unknown peaks [16]. GC/MS-coupling is employed for the identification of side products.

Working up of the electrolyte as a whole, after filtration and separation of a heavy oil phase, followed the same way as for the 10 ml samples in a 500 ml scale. In the case of the MeOH/H_2O-phase, the products were separated by fractional distillation at 10 mbar. Further details are given in [16] and Section 3.4.

3. Results

The novel anodes made of titanium, which was coated by the spinel $CoMn_2O_4$ were tested previously with the simple model Reaction 1. The more practical Reaction 2 with a higher complexity now served as a test reaction:

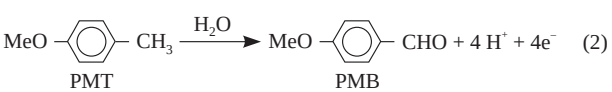

(2)

The presence of a cosolvent was necessary to achieve a homogeneous electrolyte, cf. Section 3.1. The optimum electrode coating was taken from our former work [15], cf. Section 3.2. The preparative results are discussed in Section 3.3 for the main product and for some side products, and Section 3.4 summarizes the product isolation.

3.1. *Optimization of the solvent/electrolyte system*

A cosolvent was introduced due to the limited solubility (0.01 M) of most of the aromatic compounds in pure aqueous electrolytes. Table 1 lists the systems tested. Methanol with 8 M water (entry 3) is the best. 100% MeOH is unsuitable due to heavy corrosion of the titanium substrate [17]. But 5 M H_2O, as an additive, may totally inhibit this corrosion. We used 8 M H_2O to avoid corrosion. The potential/time curves shown in Fig. 1 underlign these findings. The service life, τ, is enhanced under the present conditions in comparison to the aqueous system, where leaching experiments have shown the slow dissolution of Co and Mn, even at open circuit potential [15]. The presence of high concentrations of MeOH (> 25 M) may assist in a stabilization of the coating due to the much lower solubility of the Co and Mn components. Moreover, MeOH acts as a 'buffer', for in the absence of any PMT, the polarized anode was rather stable, and even after 1000 h, the potential had shifted positively by only 150 mV.

Table 1. Anolyte optimization for Ti/$CoMn_2O_4$ (T_a = 350 °C). Galvanostatic runs, j = 2.5 mA cm^{-2}, anodic oxidation of PMT (Equation 2)

No.	*Cosolvent*	*Anolyte composition besides 1 M H_2SO_4 and 1 M PMT*	*τ/h up to U_s = 2.5 V*
1	MeCN	MeCN, 2 M (~4%) H_2O	0.78
2	MeCN	MeCN, 8 M (~15%) H_2O	1.46
3	MeOH	MeOH, 8 M H_2O	265
4	MeOH	MeOH, 5 M H_2O	149
5	MeOH	MeOH (100%)	< 1
6	CH_3COOH	CH_3COOH (100%)	0.94

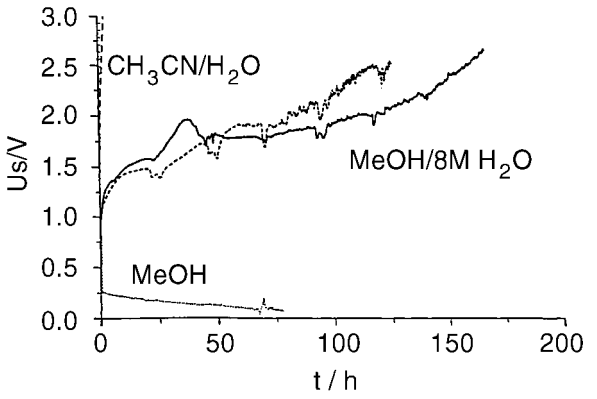

Fig. 1. Potential/time curves for the galvanostatic oxidation of 1 M PMT in 1 M H_2SO_4 in various solvents, j = 2.5 mA cm^{-2}. The anode was Ti/$CoMn_2O_4$. U_s is the potential vs Hg-l sulphate electrode in 1 M H_2SO_4, 674 mV vs SHE. Two independent runs for MeOH/8 M H_2O.

The continuous positivation of the anode potential over the service life, τ, indicates a change in surface composition. The question arises, as to whether the selectivity and current efficiency of the electrode processes change accordingly.

3.2. *Development of anode coatings*

This development was already reported in [15, 16] for aqueous 1 M H_2SO_4, with and without 1 M isopropanol. A graphical presentation of the most important results is given in Fig. 2. Clearly the spinel $CoMn_2O_4$, and its inverse spinel $MnCo_2O_4$, exhibit the longest service life values, τ.

The difference between the runs in the presence and absence of isopropanol are relatively small in spite of the fact that the electroorganic oxidation according to Equation 1 and oxygen evolution, respectively, are very different electrode processes. In contrast, the present system with the $CoMn_2O_4$ anode shows large differences between the case with and without PMT, as pointed out in Section 3.1.

Nevertheless, we have transferred the optimum experience with the $CoMn_2O_4$ spinel to the present electrode Reaction 2. The coatings were fabricated from nitrate layers by thermal decomposition in air (350 °C, 10 min) on Ti. They were found to be rather amorphous, and crystalline phases, indicated by sharp XRD peaks, were only obtained by sintering for 15 h at 650 °C [15, 16]. The coating was identified as the $CoMn_2O_4$ spinel [18]. The ASTM probe was prepared at 1000 °C [19].

3.3. *Preparative batch type electrolyses: a parametric study for the target product PMB*

The performance of the batch type electrolyses and the analytical procedure were discussed in Section 2. Table 2 summarizes the retention times, t_R, for the gas chromatographic determinations. The feedstock

Table 2. Retention times t_R in the GC for the most important electrolysis products

No.	Molecule	Acronym	t_R/s
1	*p*-methoxytoluene	PMT	308
2	3-methoxy-6-methylphenol	–	357
3	*p-tert*-butyltoluene (inner standard)	PtBT	371
4	*p*-methoxybenzylmethylether	PMBzOMe (Et*)	482
5	*p*-methoxybenzaldehyde	PMB	490
6	2,4-dimethoxytoluene	DMT	503
7	2,2′-dimethoxy-5,5′-dimethylbiphenyl	A (BP*)	800

* Used as index in Table 3.

PMT has the lowest t_R (entry 1). Products of ring oxidation (no. 2, 6), side chain oxidation (4, 5) and bimolecular ring coupling (7) are also present in the table. The distance between peaks 4 and 5 is very small, only eight seconds. Nevertheless a satisfying evaluation is possible. If the glass capillary column is coated only with crosslinked methyl silicone, without phenyl groups, both peaks coincide and separation becomes impossible.

The 2*F*-intermediate *p*-methoxy-benzylalcohol PMBzOH could not be found due to its fast oxidation to PMB. However, the formation of a methylbenzylether is possible due to the presence of methanol in a high concentration:

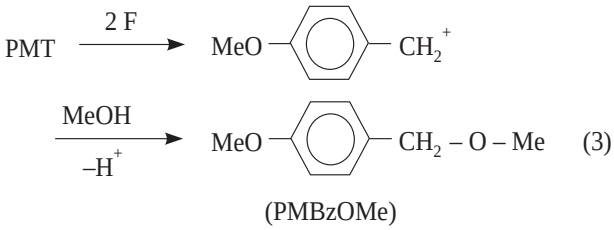

This benzylether is only slowly oxidized further; it accumulates to some extent and plays the role of an intermediate to PMA:

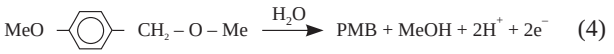

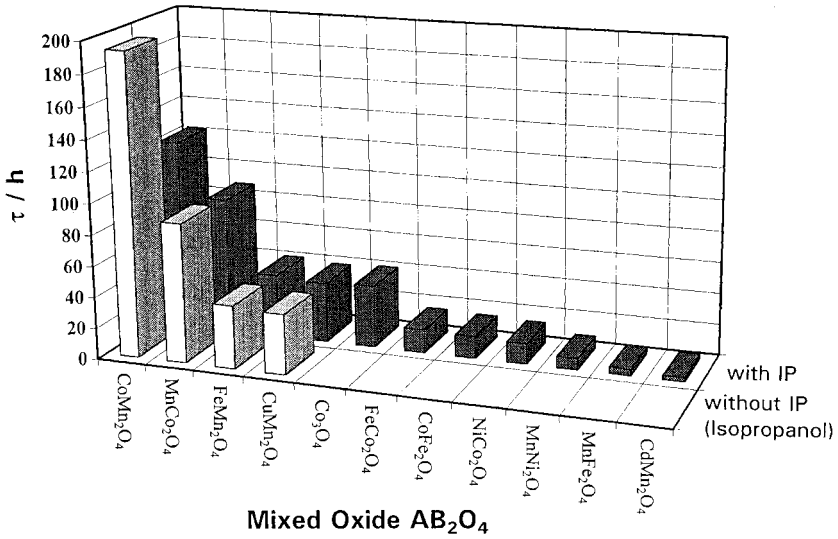

Fig. 2. Life time τ of Ti/AB_2O_4 spinel anodes at 2.5 mA cm^{-2} in dependency on the chemical composition (cf. Table 2 in [15]). Test reaction: isopropanol → acetone at 2.5 mA cm^{-2} up to U_s = 2.5 V (Fig. 1), Z_a = 3, T_a = 400 °C.

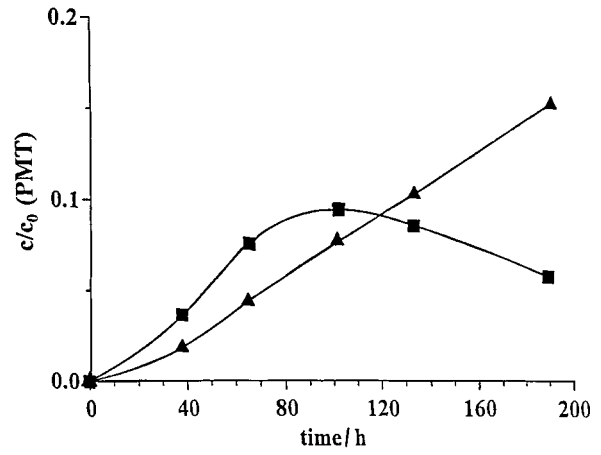

Fig. 3. Kinetic curves for the PMT oxidation at $Ti/CoMn_2O_4$ under standard conditions (Table 3). Key: (■ —— ■) ether; (▲ —— ▲) aldehyde PMB.

The kinetic curves in Fig. 3 demonstrate this behaviour. In the following, the sum of PMB and PMBzOMe is taken for the calculation of the product selectivity. Each of the batch type electrolyses were performed in two independent runs. The results were reproducible, deviations of less than 5% being observed. Table 3 shows the averaged values.

The electrolysis time under standard conditions was about 125 h (assumed consumption of 4 F per mole starting material PMT, $\beta_{th} = 30\%$). However, Table 3 reveals that reaction rate for PMT consumption was appreciably higher due to the formation of benzylmethylether (Et) according to Equation 3 and the formation of biphenyls (BP), consuming only 2 and 1 F per mole starting material, respectively. The latter side reaction predominantly yields the following isomer, (cf. [20], and see no. 7 in Table 2):

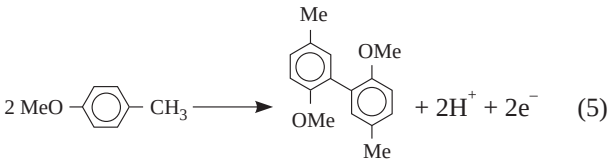

(5)

The C—C bond is in the α-position of the methoxy groups. This is concluded from electronic considerations, according to which the rearomatization of the dimers is faciliated by this kind of coupling [16]. Table 3 includes data for this quantitatively prevailing dimer side product with the index 'BP'. A third and fourth category of side products have their origin in the nuclear substitution reactions of the monomers and dimers (biphenyls). Typical examples for the monomer substitution products, which are present in higher quantities, are 2,4-dimethoxytoluene and 3-methoxy-6-methylphenol. The equation for the former is

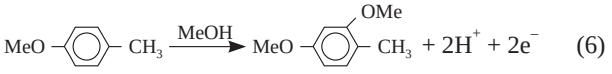

(6)

These side reactions again consume less electricity, namely 2 F per mole starting material.

Table 3. Results of the GC-analysis

Standard: $c_{PMT} = 1$ M, n_o, (PMT) = 500 (100 for no. 6, 50 for no. 7) mmol, 1 M H_2SO_4/MeOH, $V_0 = 0.5$ l, $\beta_{th} = 30\%$ (4 F), $j = 2.5$ mA cm^{-2}, $T = 23$ °C, $Ti/CoMn_2O_4$-anode, $A = 50$ cm^2

No.	Deviation from standard	c_W /M	Cell	a n_{ET} /mmol	b n_{PMB} /mmol	c n_{BP} /mmol	d CE_{Et} /%	e CE_{PMB} /%	f CE_{BP} /%	g SE_{Et} /%	h SE_{PMB} /%	i SE $(ET + PMB)$/%	k SE_{BP} /%	l SE_M /%	m SE_D /%	n $CONV$ (PMT)/%
1	–	8	D	47	53	8.8	16	35	2.9	15	18	**33**	6	5	8	61
2	$c_W = 5$ M	5	D	62	38	7.3	21	26	2.9	21	18	**45**	7	4	10	45
3	Cell = Q	8	Q	75	31	9.6	26	22	3.3	35	14	**49**	9	2	9	44
4	$j = 5$ mA cm^{-2}	8	D	53	30	19	19	21	6.5	22	13	**35**	6	6	13	54
5	$T = 50$ °C	5	Q	65	18	10	22	12	3.5	28	8	**36**	8	3	12	45
6	$c_{PMT} = 0.2$ M	5	Q	12	8	1.8	21	29	3.2	36	24	**60**	10	2	8	34
7	$c_{PMT} = 0.1$ M	5	Q	5	6.8	0.6	18	47	1.9	20	34	**54**	4	1	4	43
8	Isopropanol instead of MeOH	5	D	31	30	10	10	20	3.4	19*	19	**38**	12	4	11	34
9	Pt-anode	8	D	65	17	13	23	12	4.5	24	7	**32**	9	6	7	55
10	Pb/PbO_2-anode	5	Q	15	1.5	19	5.2	1.1	10	9	1	**10**	22	5	11	37

* including the free benzylalcohol, ~1%

CONV = conversion, CE = current efficiency, SE = selectivity, D = divided cell, Q = quasidivided cell, c_W = water concentration, β_{th} = theoretical conversion under ideal conditions.

Table 3 contains three main current efficiencies CE (columns d–f) derived directly from the measured product mole numbers n (columns a–c). In addition, six selectivities, SE, are compiled (columns g–m). The ether ($2\,F\,mol^{-1}$) and the aldehyde ($4\,F\,mol^{-1}$) represent the main product, and the sum of both are given in column i. SE_{BP} shows the selectivity for the dominating side reaction for the biphenyl derivative according to Equation 5. SE_D are estimated for other dimers from the GC-results, as SE_M for other monomer products (cf. Equation 6). The final column (n) stands for the conversion of PMT. The reasons for the enhanced conversions (34–61% rather than 30%) were discussed above.

The results under standard conditions are displayed as entry 1. The formation of ether increases at lower water concentrations, cf. entry 2. This may be a consequence of a lower rate of the formation of OH-radicals at the anode, which may initiate polymerizations. An additional decrease of c_W beyond 5 M is not possible due to the instability of the Ti substrate, as already mentioned [17]. The application of a quasidivided cell Q (entry 3) leads to improved selectivity. This may be attributed to the rereduction of some of the oxidative intermediates, which may have led otherwise to irreversible sideproducts. Entry 4 shows that a twofold current density leads to nearly the same selectivity, but the CE and therefore the space time yield is appreciably lowered. As already mentioned, electrode life is also lowered. The dimer products increase to some extent as a consequence of an enhancement of the bimolecular pathways. A temperature of 50 °C (entry 5) gives the same selectivity, but much more of the ether is formed. A chemical step such as $R\cdot^{+} + CH_3OH$ may be rate determining.

Optimum results are obtained at lower educt concentrations, 0.1 and 0.2 M, (cf. entries 6 and 7). The selectivities reach 60%, and the current efficiencies 50%. The bimolecular side product pathways are greatly inhibited. A drawback, of course, is the larger effort for working up steps. Quasicontinuous electrolyses at these concentrations confirm these findings; the combined selectivities are only slightly diminished. This may be a consequence of the constancy of the initial educt concentration, c_0, in case of the quasicontinuous mode, but a decrease of c_0 in the course of a batch type electrolysis occurs. If isopropanol is employed instead of methanol (cf. entry 8), the selectivities for the main products remain unchanged, but SE_{BP} and SE_D become large, and CE for the desired products drop from 50 to 30%. This is a consequence of the enhanced anodic oxidation of the alcohol. A small amount of the free benzyl alcohol was identified for the first time. The reason is the sluggish kinetics for ether formation with isopropanol.

Finally, the substitution of the novel anode Ti/$CoMn_2O_4$ by the conventional anodes Pt and PbO_2 was tested. Platinum (entry 9) yields a similar SE, but with a much higher ether portion. The CEs are only 35%. Pt as anode for the oxidation of PMT under slightly different conditions (0.5 M PMT in 0.05 M H_2SO_4) acetone cosolvent (1:1 v/v, $j = 50\,mA\,cm^{-2}$, 6 °C) gave no PMA, but a diphenylether derivative (5.4′-dimethyl-2-methoxy-diphenyl ether) is obtained in high yields, 36–88%, according to the work of Hlavaty [21]. Lead dioxide (entry 10), however, is much inferior. SE drops to 10%, and CE to 6%. Interestingly, SE_{BP} for the specific dimer after Equation 5 is relatively high, and this electrosynthesis could be useful for this product, which is otherwise not easily accessible.

It should be noted that attempts to work in pure aqueous emulsions failed due to an extremely short electrode service life of only 9.5 h. We conclude from this surprising finding that the alcoholic cosolvent plays an important role for the stabilization of the active layer (cf. Section 3.2).

3.4. *Product isolation*

The aim of this part of the work was twofold: to gain information about (a) possible working up procedures and (b) about those products, originating from PMT, which could not be separated or identified by GC. The electrolyte separates after electrolysis into a heavy oil as the lower phase (I) and a clear upper phase (II). Each phase contains about 50% of that 20–50% unknown (polymer and oligomer) components, which follow from the deficit of fractions which were compiled in the selectivity columns i–m in Table 3 up to 100%.

From phase I, yellow solids were separated by the addition of hexane to the solution in Et_2O. Phase II yields, after neutralization with 2 M NH_3 and stripping of the methanol, a solution which was extracted by Et_2O (cf. paragraph 2). The ether was removed by stripping, and the oil phase was distilled in vacuum. The products were separated up to 1 torr/74 °C. The nondistillable residue corresponded to oligomers and polymers. Clearly, (I) and (II) are minimized to about 10% by working at low educt concentrations (0.1–0.2 M), cf. entry 6 in Table 3.

4. Conclusions

This work extends our knowledge about the possibilities of electrodes with surface fixed redox systems to realize heterogeneous redox catalysis. A general review in this field was given formerly [35, 36]. Other examples, not based on Mn, which focus on the selective anodic oxidation of aromatics, are shown in Table 4.

The spinel $CoMn_2O_4$ yields an 'island of stability' in acid solutions (Fig. 2). Most spinels dissolve under such conditions, at least partially, and are not stable at high pH-values [37]. Other applications for $CoMn_2O_4$ are also reported, for example, as host lattices in rechargeable Li-batteries [39].

The unexpected stability of the novel anodes seems to be correlated to the structural aspect, that octa-

Table 4. Composite anodes for the oxidation of aromatic compounds

Coating	*Substrate*	*Educt*	*Solvent/electrolyte system*	*References*
PbO_2	Pb, Ti	*t*-butyltoluene	e.g. $H_2O/CH_2Cl_2/H_2SO_4$ (emulsion)	[22–24]
PbO_2 + chloride	Pb	*t*-butyltoluene		[25]
PbO_2 + Bi (III)	Pb	*t*-butyltoluene		[26]
Cr_2O_3	Ti	ethylbenzene	1 M H_2SO_4 + cosolvent	[7, 27, 28]
Cr_2O_3	graphite	*t*-butyltoluene	H_2O + CH_3COOH + $NaBF_4$	[29, 30]
RuO_2	Ti	*p*-methoxytoluene	acetate buffer	[31]
RuO_2	Ti	benzylalcohol		[32]
Me-sulphides, -carbides	C, Ti	aromatics		[33]
Polymerbound redoxsystem	C, Ti	aromatics		[34]

hedral sites B in AB_2O_4 are occupied by Mn species in two oxidation states, Mn^{3+} and Mn^{4+} [39–48]. Further structural details can be found in [49–54]. This supports also the mechanism via heterogeneous redox catalysis. The electrochemical step, E, leads to Mn^7 species at the surface:

$$\underset{\text{Red}}{\overset{2}{\text{Co}}\,\overset{3}{\text{Mn}}_2\,\text{O}_4} + 4\text{H}_2\text{O} \xrightarrow{\text{E}} \underset{\text{Ox}}{\overset{2}{\text{Co}}\,\overset{7}{\text{Mn}}_2\,\text{O}_8} + 8\text{H}^+ + 8\text{e}^- \tag{7}$$

Three chemical follow-up steps C depart from this centre, namely, (i) the oxidation of the aromatic molecule, (ii) the generation of O_2 [55–58] and (iii) the dissolution of permanganate ions. Their characteristic colour is visible in the diffusion layer. (iii) represents the irreversible wearing process of the anode. The turnover factor, f_{to} of the oxide coating is found to be 2.200.

$$f_{to} = \frac{\tau j}{zFV_{A,Pr}c_{Pr}Z_a} \tag{8}$$

($V_{A,Pr}$ = volume per area of the precursor solution of concentration, c_{Pr}, Z_a = number of thermal cycles). It is larger by a factor four than in the Cr_2O_3/CrO_3 system [28], $Cr_2O_3/Sb_2O_3/TiO_2$. However, it should be mentioned that screening of the oxide composition was not yet performed for the present model Reaction 2.

A typical effect for the presence of redox catalysis is the current amplification, f_a, in the presence of a depolarizer. Figure 4 shows a characteristic example: $f_a = 2$. For isopropanol oxidation at the same anode, $f_a \sim 1$ [15, 16], and of Ti/Cr_2O_3, $f_a \sim 10$. Thus, the f_a factors can be derived from quasisteady state current voltage curves.

A positive shift of the anode potential of $Ti/CoMn_2O_4$ is observed during current flow due to the consumption of the coating. The question of how this influences the differential values of CE and SE should be discussed briefly. In the case of isopropanol oxidation in aqueous H_2SO_4, the main reaction proceeds according to Equation 1, and the SE and CE coincide only at the beginning at about 100%. Later, the CE decreases continuously due to oxygen evolution in parallel, which becomes possible at the positive potentials.

Interestingly, the electrode life in the absence of the alcohol is nearly the same Fig. 2. As already mentioned, f_a is about 1. In the case of PMT oxidation to PMB, according to the overall Equation 2, SE and CE remain constant during the whole electrolysis time, albeit at a relatively low level. As the anode potential is shifted again into the positive direction a

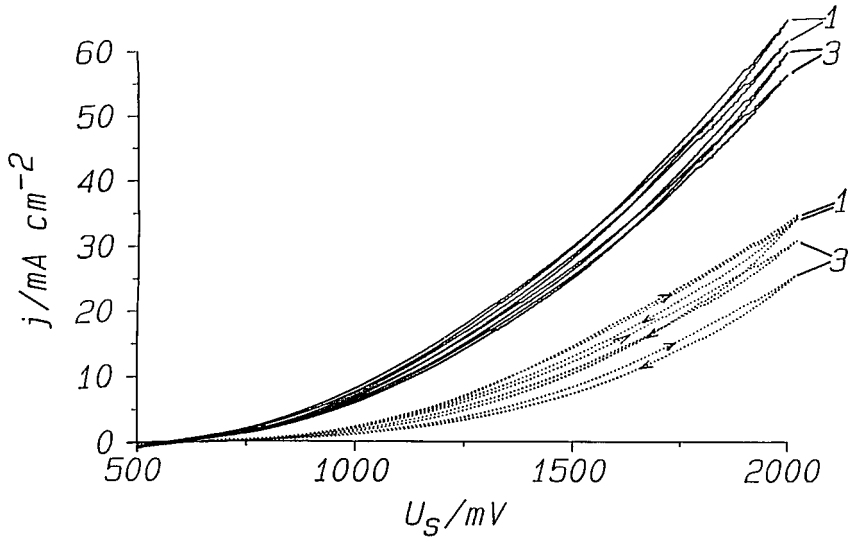

Fig. 4. Current/voltage curves, 10 mV s^{-1}, $Ti/CoMn_2O_4$. Electrolyte: 1 M H_2SO_4/8 M H_2O/MeOH. Two independent runs: 1 and 3 cycles (------) without PMT and (——) with 1 M PMT. U_s (V vs Hg-I sulphate electrode).

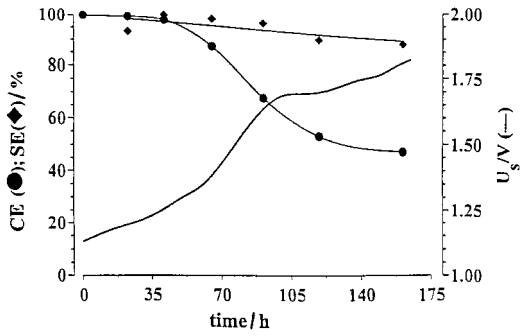

Fig. 5. Selectivity SE and current efficiency CE for the anodic oxidation of 1 M isopropanol in 1 M H_2SO_4 at 2.5 mA cm^{-2}. Anode: Ti/$CoMn_2O_4$; $\beta_{IP} \sim 50\%$ after 165 h.

change of surface composition must be concluded as before, but without a strong influence on these parameters. They are decoupled from the beginning. This may be a consequence of the parallel reaction, the oxidation of methanol.

The reaction mechanism of Reaction 2 may be summarized according to Fig. 7. The main route (in the middle) consists of a couple of follow up reactions. The first one electron step leads to the very reactive radical cation. The benzyl alcohol is not identified in spite of the presence of 5 (8) M H_2O, due to the fast oxidation to the aldehyde. The side reactions at the right proceed via side chain oxidation with CH_3OH- or H_2O-reaction partners. The benzylmethyl ether is built up among other due to the sluggish further oxidation to the aldehyde (Fig. 3). The left part represents the formation of dimers and oligomers through oxidative C—C-coupling at the aromatic ring.

The adsorption of organic components plays an important role, as in many other examples in organic electrosynthesis [59, 60]. This is supported by the inferior preparative results, if the starting material PMT is substituted by *p-tert*-butyltoluene. Under the otherwise identical standard conditions as in Table 3 a conversion of only 10% was found. The benzylalcohol could be identified this time, but only with 3%

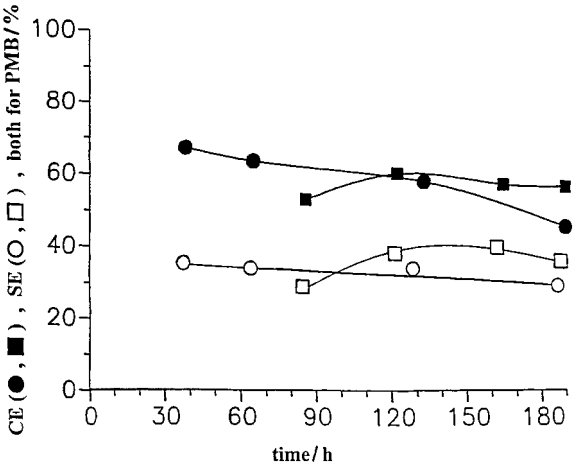

Fig. 6. SE and CE (as in Fig. 5) for the anodic oxidation of 1 M PMT in 1 M H_2SO_4/8 M H_2O in methanol at 2.5 mA cm^{-2}. Anode: Ti/$CoMn_2O_4$; $\beta_{4F} = 30\%$ after 125 h. Two independent runs.

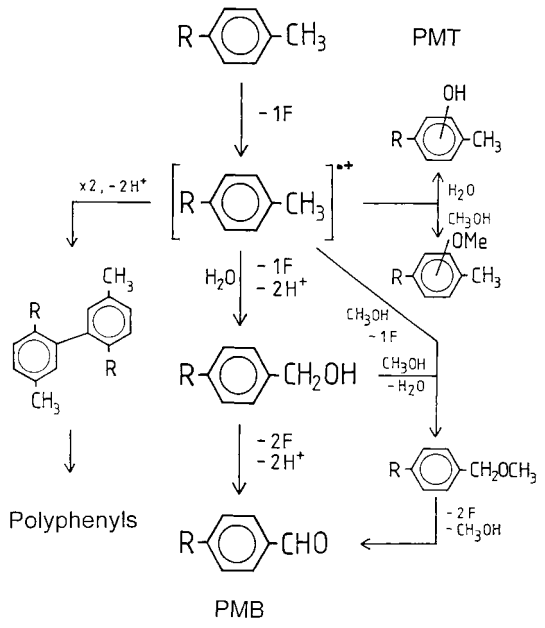

Fig. 7. Mechanism of the anodic oxidation of PMT to PMB at Ti/$CoMn_2O_4$.

selectivity. Our experimental findings allow for the establishment of the following sequence of competitive adsorption

$$\text{PMB} > (\text{PMB})_{\text{MeOH}} > \text{MeOH} > \text{H}_2\text{O} > (\textit{p-tert}\text{-butyltoluene})_{\text{MeOH}}$$

Finally, the low current densities necessitate the use of cells with a high space time yield such as the capillary gap cell [61–63] or the Swiss roll cell [64–66].

Acknowledgements

We thank Dr B. Wermeckes of this laboratory for his assistance in the solution of preparative and analytical problems. One of us (E.L.) is indebted to the University of Duisburg for financial support. The provision of titanium sheet by Thyssen AG and of PMT/PMB by BASF AG is gratefully acknowledged.

References

[1] D. Pletcher and F. C. Walsh, 'Industrial Electrochemistry', 2nd edn, Chapman & Hall, London (1989).
[2] D. Degner, *Top. Current Chem.* **148** (1988) 1–95.
[3] F. Beck, *Kagaku to Kogyo* **43** (12) (1990) 1997.
[4] German Patent *2 848 397* (BASF, D. Degner, M. Barl and H. Hannebaum, 1978).
[5] F. Beck, B. Wermeckes and Siyu Ye, *DECHEMA Monographs* **125** (1992) 753.
[6] H. Beer, GDR-Pat. *55 223* (prior. date 12.5.1965), Belgium-Patent *710 551* (2/67).
[7] F. Beck and H. Schulz, *Electrochim. Acta* **29** (1984) 1569.
[8] B. Wermeckes and F. Beck, *ibid.* **30** (1985) 1491.
[9] J. P. Millington, A. R. Jones, A. J. Hughes and J. E. Trotman, British Patent *2 164 935* (1986).
[10] Ch. Comninellis, *J. Electrochem. Soc.* **129** (1992) 749.
[11] *Idem*, *J. Appl. Electrochem.* **17** (1992) 1315.
[12] L. Eberson and K. Nyberg, *J. Am. Chem. Soc.* **88** (1966) 1686.
[13] *Idem*, *Acc. Chem. Res.* **6** (1973) 106.
[14] A. Nilsson, V. Palmquist, T. Petterson and A. Ronlan, *J. Chem. Soc., Perkin Trans. I* **1978** 708.
[15] E. Lodowicks and F. Beck, *Chem. Engng Techn.* **17** (1994) 338.

[16] E. Lodowicks, PhD thesis, University of Duisburg (1996).
[17] L. D. Burke, J. F. Healy and O. J. Murphy, *J. Appl. Electrochem.* **13** (1983) 469.
[18] 'Powder Diffraction File', edited by Joint Committee of the Powder Diffraction Standards (JCPDS), Swarthmore, PA (1974).
[19] G. Prokhvatilov, *Sov. Phys. Crystallogr.* **10** (1965) 191.
[20] G. Kreysa and H. Medin, *J. Appl. Electrochem.* **16** (1986) 557.
[21] J. Hlavaty, *J. Appl. Electrochem.* **24** (1994) 989.
[22] P. Seiler, EP *30 588* (1981).
[23] J. S. Clarke, R. E. Ehigamusoe and A. T. Kuhn, *J. Electroanal. Chem.* **70** (1976) 333.
[24] J. P. Millington, Swiss Patent *597 369* (1978).
[25] Y.-L. Hsiao and D. C. Johnson, *J. Electrochem. Soc.* **136** (1989) 3704.
[26] I.-H. Yeo and D. C. Johnson, *ibid.* **134** (1987) 1973.
[27] F. Beck and H. Schulz, *Ber. Bunsenges. Phys. Chem.* **88** (1984) 155.
[28] F. Beck and H. Schulz, *J. Appl. Electrochem.* **17** (1987) 914.
[29] D. Degner and H. Siegel, DE *2 855 508* (1980).
[30] D. Degner, H. Roos and H. Hannebaum, EP *72 914* (1983).
[31] M. A. Halter and T. P. Malloy, US *212 710* (1980).
[32] S.-M. Lin and T.-C. Wen, *J. Appl. Electrochem.* **25** (1995) 73.
[33] D. Degner, H. Ross and H. Hannebaum, DE *3 132 726* (1982).
[34] J. Yoshida and K. Ogura, *J. Org. Chem.* **49** (1984) 3419.
[35] F. Beck, W. Gabriel and H. Schulz, *DECHEMA Monographs* **102** (1986) 339.
[36] F. Beck, B. Wermeckes and E. Zimmer, *ibid.* **112** (1988) 257.
[37] M. R. Tarasevich and B. M. Efrimov, Properties of Spinel-type Oxide Electrodes, *in* 'Electrodes of Conductive Metal Oxides' Vol. A (edited by S. Trasatty), Elsevier, Amsterdam (1980).
[38] J. Farcy, J. P. Pereira-Ramos, L. Hernan, J. Morales, J. L. Tirado, *Electrochim. Acta* **39** (1994) 339.
[39] P. J. Wojtowicz, *Phys. Rev.* **116** (1959) 32.
[40] M. Rosenberg and P. Nicolau, *Phys. Stat. Sol.* **6** (1964) 101.
[41] B. Boucher, R. Buhl and M. Berrin, *Acta Crystallogr.* **25** Sect. B (1969) 2326.
[42] J. P. Brenet and J. F. Koenig, *Z. Phys. Chem.* **98** (1975).
[43] J. P. Brenet, *Power Sources* **4** (1979) 183.
[44] J. L. Gautier, R. Fuentealba and C. Cabezas, *Z. Phys. Chem.* **126** (1981) 71.
[45] V. A. M. Brabers and J. C. M. Terhell, *Phys. Stat. Sol.* **A 69** (1982) 325.
[46] J. L. Gautier and C. Cabezas, *J. Electroanal. Chem.* **159** (1983) 137.
[47] M. Lenglet, J. Lupitaux and R. Guillamet, *Mater. Chem. Phys.* **14** (1986) 199.
[48] E. D. Macklen, *J. Phys. Chem. Solids* **47** (1986) 1073.
[49] J. Goodenough, *J. Phys. Rad.* **20** (1959) 155.
[50] G. H. Jonker and S. van Houten, *Halbleiterprobleme* **6** (1961) 118.
[51] P. Scheftel, *Sov. Phys. Sol. State* **7** (11) (1966) 2781.
[52] B. Boucher, R. Buhl and M. Perrin, *J. Appl. Phys.* **39** (1968) 632.
[53] A. Meenakshisundaram, N. Gunasekaran and V. Srinivasan, *Phys. Stat. Sol* **A 69** (1982) K 15.
[54] A. Feltz and M. Ottlinger, *Z. Chem.* **29** (1989) 338.
[55] F. Haber and S. Ginsberg, *Z. Anorg. Allg. Chem.* **18** (1988) 37.
[56] G. Grube, *Z. Elektrochem.* **33** (1927) 389.
[57] R. Kötz, H. J. Lewerenz, P. Brüesch and S. Stucki, *J. Electroanal. Chem.* **150** (1983) 209.
[58] P. Rasiyah and A. C. C. Tseung, *J. Electrochem. Soc.* **131** (1984) 803.
[59] H. Wendt, *Chem. Ing. Tech.* **45** (1973) 1303.
[60] *Idem*, *J. Mol. Catal.* **38** (1986) 89.
[61] F. Beck and H. Guthke, *Chem. Ing. Tech.* **41** (1969) 943.
[62] F. Beck, *Electrochim. Acta* **18** (1973) 359.
[63] *Idem*, Pure Appl. Chem. Spec. Suppl. XXIV. IUPAC Congr. **5** (1974) 111.
[64] P. M. Robertson, P. Cettou, D. Matie, F. Schwager, A. Storek and M. Ibl. *AlChE Symposium Series* **185** 75 (1979) 115.
[65] P. Seiler and P. M. Robertson, *Chimia* **36** (1982) 305.
[66] R. Roberts, R. P. Ouellette and P. N. Cheremisinoff, 'Industrial Applications of Electroorganic Synthesis', Ann Arbor Science Publishers, MI (1982).